Identification of incident seismic wave in time domain considering non-linear behavior of soil

H.Sakai
Wakachiku Construction Corporation Ltd., Tokyo, Japan
S.Sawada
Disaster Prevention Research Institute, Kyoto University, Uji, Japan
K.Toki
Graduate School of Civil Engineering, Kyoto University, Kyoto, Japan

ABSTRACT: Incident seismic wave to the base layer is necessary for computing the response of soil and structure system. In most cases, the incident wave has been calculated in frequency domain based on the multiple reflection theory from the observed records on the ground surface or in the borehole and the equivalent linear model has been employed to approximate the non-linear behavior of soil. However it is not acceptable for simulations of seismic behavior of structures under strong shaking, particularly, when we discuss the residual deformation or collapse of structures. In this paper, the formulation of the backward calculation method is proposed to identify the incident seismic wave considering non-linear behavior of ground. The numerical properties of the method are shown based on the modal analysis. Numerical examples are conducted to examine the accuracy and stability of the method.

1 INTRODUCTION

Non-linear Finite Element models are often employ-ed to analyse the dynamic soil-structure interaction. An incident seismic wave on the base layer is necessary for analysing earthquake responses using FEM model. The incident wave is frequently identified using the observed records on the ground surface or in the borehole as shown in Fig.1.

The identification methods of the incident wave can be classified roughly into two methods; one in frequency domain and one in time domain. The former is mostly performed with a typical conven-tional linearization program, “SHAKE” (Schnabel et al. 1972). This program is based on the equivalent linear model to approximate the non-linear behavior of soil. Even if the incident wave is identified from the observed record on ground surface by making use of the equivalent linear model and the earth-quake response of the ground is analysed by non-linear model, the calculated wave form on ground surface do not usually coincide with the observed record. Namely, the earthquake response analysis is performed under the different condition where the record had been observed. Then the incident wave is needed to identify the ground motion using the same

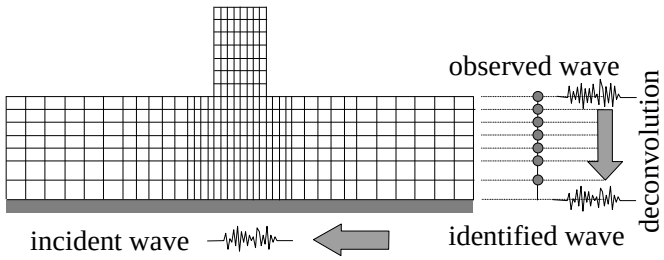

Figure 1 Procedure of soil-structural dynamic analysis

non-linear model as the forward analysis to improve this problem. Therefore the identification should be done in the time domain.

There are several studies of the identification of the incident seismic wave in time domain. Input ground motions of structural systems with linear re-storing properties were identified under the assump-tion of three degree of freedom (3DOF) by making use of the Kalman filter (Toki et al. 1989) and by the EK-WLI method (Sudo et al. 1995). Maruyama & Hoshiya (1987) proposed the formulation for identification of non-linear single degree of freedom (SDOF) systems. However, these analyses have been practically performed using linear systems. The identification method of the incident seismic wave using non-linear system is not established yet.

In this paper, a new method to identify the inci-dent seismic wave in time domain considering non-linear behavior of soil is proposed. At first, a formu-lation

of the backward calculation method is shown, which is applicable for a multidegree of freedom (MDOF) non-linear system. Next, the numerical characteristics of the method are shown based on the modal analysis and numerical examples. Lastly, the method is modified using the penalty function to reduce the numerical error of the method.

2 BACKWARD CALCULATION METHOD

2.1 *Equation of motion*

The equation of motion of a MDOF system with a non-linear stiffness can be written as

$$\boldsymbol{M}\ddot{\boldsymbol{x}}^n + \boldsymbol{C}\dot{\boldsymbol{x}}^n + \boldsymbol{K}\boldsymbol{x}^n - \boldsymbol{Q}^n = -\boldsymbol{M}\boldsymbol{i}\ddot{z}^n \qquad (1)$$

where $\boldsymbol{M}$, $\boldsymbol{C}$ and $\boldsymbol{K}$ are mass, viscous damping and stiffness matrices of the system, respectively, $\boldsymbol{x}$ nodal displacement vector, $\boldsymbol{Q}$ a quasi-external force vector which can be considered as additional external forces to make the linear system equivalent to the non-linear system, $\boldsymbol{i}$ a vector of which all components are 1, $\ddot{z}$ incident acceleration, dot (•) a time derivation and superscript n represents the number of time steps.

In a case that the absolute acceleration of mass k at n-step, $\ddot{y}_k^n$, is observed, it is related with $\ddot{z}^n$ and $\ddot{x}_k^n$ as follows:

$$\ddot{z}^n = \ddot{y}_k^n - \ddot{x}_k^n \qquad (2)$$

where subscript k denotes the mass number.

The following equation is given by substituting Eq.(2) into Eq.(1):

$$\boldsymbol{M}'\ddot{\boldsymbol{x}}^n + \boldsymbol{C}\dot{\boldsymbol{x}}^n + \boldsymbol{K}\boldsymbol{x}^n - \boldsymbol{Q}^n = -\boldsymbol{M}\boldsymbol{i}\ddot{y}_k^n, \qquad (3)$$

in which,

$$M'_{ij} = M_{ij} - \sum_{l=1}^{N} M_{il}\delta_{jk}, \qquad (4)$$

where M'_{ij} and M_{ij} are ith-row and jth-colomn components of $\boldsymbol{M}'$ and $\boldsymbol{M}$, respectively, δ_{ij} is Kronecker's delta, N denotes number of freedom.

2.2 *Time integration method*

Newmark-b method is applied for integrating Eq.(3) in time domain to obtain the time histories of the response vectors. It assumes the following relations;

$$\dot{\boldsymbol{x}}^{n+1} = \dot{\boldsymbol{x}}^n + (1-g)\Delta t\ddot{\boldsymbol{x}}^n + g\Delta t\ddot{\boldsymbol{x}}^{n+1}, \qquad (5)$$

$$\boldsymbol{x}^{n+1} = \boldsymbol{x}^n + \Delta t\dot{\boldsymbol{x}}^n + \frac{1}{2}\Delta t^2\ddot{\boldsymbol{x}}^n + b\Delta t^2(\ddot{\boldsymbol{x}}^{n+1} - \ddot{\boldsymbol{x}}^n), \qquad (6)$$

where, Δt is time increment, g and b are parameters which govern the stability and numerical dissipation of the algorithm.

Eq.(7) is given by substituting Eqs.(5) and (6) into Eq.(3).

$$\ddot{\boldsymbol{x}}^{n+1} = \boldsymbol{A}^{-1}\boldsymbol{b} \qquad (7)$$

in which

$$\boldsymbol{A} = \boldsymbol{M}' + g\Delta t\boldsymbol{C} + b\Delta t^2\boldsymbol{K} \qquad (8)$$

$$\boldsymbol{b} = -\boldsymbol{M}\boldsymbol{i}\ddot{y}_k^{n+1} + \boldsymbol{Q}^{n+1} + \boldsymbol{C}(\dot{\boldsymbol{x}}^n + (1-g)\ddot{\boldsymbol{x}}^n) + \boldsymbol{K}(\boldsymbol{x}^n + \Delta t\dot{\boldsymbol{x}}^n + (1/2 - b)\Delta t^2\ddot{\boldsymbol{x}}^n) \qquad (9)$$

The incident acceleration is obtained from Eq.(2), if $\ddot{x}^{n+1}$ is given by Eq.(7). As $\boldsymbol{Q}^{n+1}$ in Eq.(7) is related with $\boldsymbol{x}^{n+1}$, the iterative calculation is needed to satisfy the equilibrium at (n+1)-step.

3 CHARACTERISTIC OF BACKWARD CALCU-LATION METHOD

3.1 *Eigen values*

Although the equation of motion of the backward calculation, Eq.(3), is the same type as that of the forward calculation, Eq.(1), the terms of the mass matrix and the external force are different. A property of the backward calculation method is investigated by eigen value analysis using the equation of free oscillation.

A 3DOF viscous damping system is adopted for the analysis whose matrices are given by

$$\boldsymbol{M} = \begin{bmatrix} m_1 & 0 & 0 \\ 0 & m_2 & 0 \\ 0 & 0 & m_3 \end{bmatrix}, \boldsymbol{C} = \begin{bmatrix} c_1 & -c_1 & 0 \\ -c_1 & c_1 + c_2 & -c_2 \\ 0 & -c_2 & c_2 + c_3 \end{bmatrix},$$

$$\boldsymbol{K} = \begin{bmatrix} k_1 & -k_1 & 0 \\ -k_1 & k_1 + k_2 & -k_2 \\ 0 & -k_2 & k_2 + k_3 \end{bmatrix}.$$

By replacing the right hand side of Eq.(3) by **0**, the equation of free oscillation of the backward calcu-lation method is obtained. The eigen values and vectors of the equation are obtained and shown in Table 1.

In the forward analysis, the eigen values of the equation are complex numbers in general and this shows that the system vibrates on the eigen modes with damping. However, as shown in Table 1, the eigen values of the backward calculation are negative real numbers and its absolute values are large, because k_i is generally much greater than c_i. Then a rigid mode exists as one of the eigen vectors.

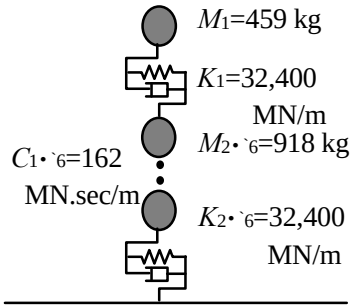

Figure 2.1 Linear 6DOF model

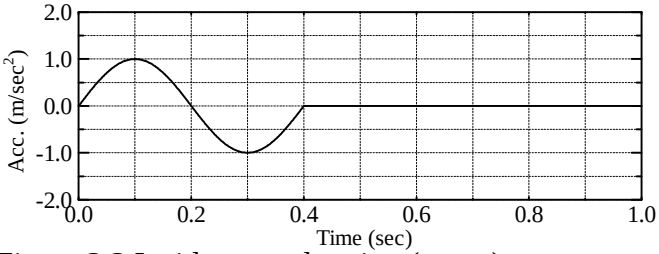

Figure 2.2 Incident acceleration (target)

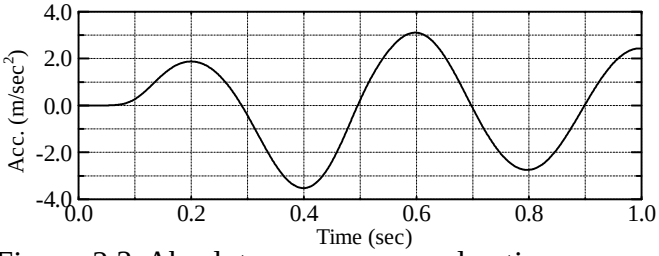

Figure 2.3 Absolute response acceleration curve at the top mass computed by the forward calculation

Table 1 Eigen value l and eigen vector $\boldsymbol{u}$ of 3DOF free vibration system of equation (3)

l	$\boldsymbol{u}$
$-\frac{k_1}{c_1}$	$\begin{Bmatrix} (m_2k_1^2 - c_1c_2k_1 + c_1^2k_2)(m_3k_1^2 - c_1c_3k_1 + c_1^2k_3) + m_2(c_1k_2 - c_2k_1)c_1k_1^2 \\ (m_2+m_3)(c_1k_2 - c_2k_1)c_1k_1^2 + m_2m_3k_1^4 \\ (m_2+m_3)(c_1k_2 - c_2k_1)c_1k_1^2 + m_2(m_3k_1^2 + c_1k_3 - c_3k_1)k_1^2 \end{Bmatrix}$
$-\frac{k_2}{c_2}$	$\left\{1 \quad 1 \quad \frac{m_3k_2^2}{m_3k_2^2 - c_2c_3k_2 + c_2^2k_3}\right\}^T$
$-\frac{k_3}{}$	$\{1 \quad 1 \quad 1\}^T$

Therefore, the system has over damping properties and the response amplitudes of the system decrease rapidly including the rigid mode. A system with large number of freedom should have the same properties. Namely, when the calculation error is occurred in the backward calculation, it causes a vibration with over damping including a rigid mode. The eigen modes are not orthogonal each other and the number of eigen values and vectors are not always the same number as freedoms, because the matrices in the equation are not symmetric.

3.2 *Effect of integration parameter b*

The effect of integration parameter b is examined by numerical examples using a 6DOF linear system. The model and its parameters are shown in Fig.2.1. The incident motion is one cycle of sinusoidal wave with the period of 0.4 second. The absolute response acceleration at the top mass is calculated. These wave forms are shown in Figs.2.2 and 2.3, respectively.

Identification of the incident wave is performed in 6 cases of b=1/2,1,2,3,10,20. Other parameters are set to Δt=1/1000 second and g=1/2. Fig.2.4 shows the identified incident accelerations. In the case of b=1/2, divergence occurs at several tens of time steps. In the case of b=1, the identified incident wave almost consists of large amplitude and high frequency errors. In the case of b=2 the errors in high frequency component become small, and in case of b=3 the identified incident acceleration is almost same as the target. In this case, maximum calculation error determined by the following equation is 5.1%.

$$\text{max. calculation error} = \frac{\left|(\text{identified}) - (\text{exact})\right|_{\max}^{t=0\sim N\Delta t}}{\left|(\text{exact})\right|_{\max}^{t=0\sim N\Delta t}}$$

In section 3.1, the characteristic of the backward calculation method is investigated by making use of the modal analysis. Here, it is also examined by the numerical example. Fig.2.5 shows the calculation error of the relative response acceleration of each mass in the case of b=1/2. It is observed from the figure that the calculation errors consist of high frequency vibration of the rigid mode.

In the forward analysis, value of b is usually chosen from 0 to 1/4 and, therefore, it seems to be unusual for adopting b=2 or 3 which is suggested by the examination compared in Fig.2.4. Because it has been considered that the damping of the system is overestimated and the accuracy of the solution gets worse when b is greater than 1/4. In the forward analysis, the accuracy of the forward analysis is examined for b and Δt. The same model is used as the previous one shown in Fig.2.1. Its shortest eigen period is 5/100 second and the El Centro(1940) NS component is used as the incident wave. Table 2

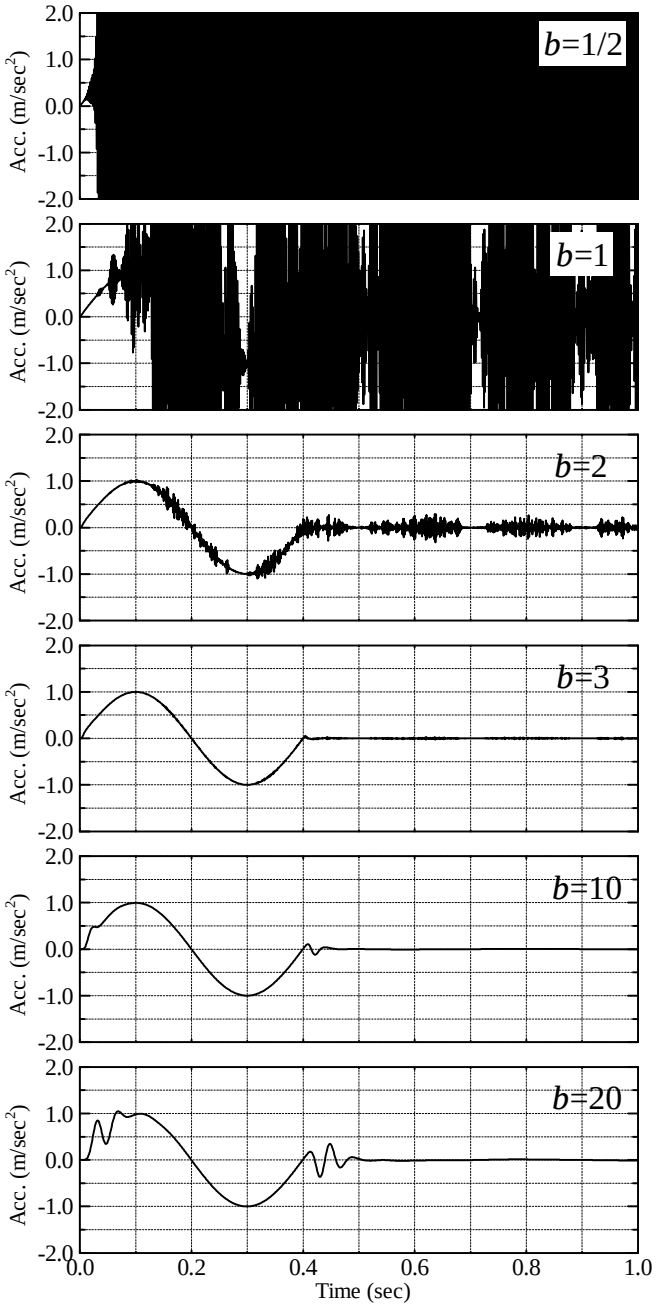

Figure 2.4 Effect of b on identified incident accelerations

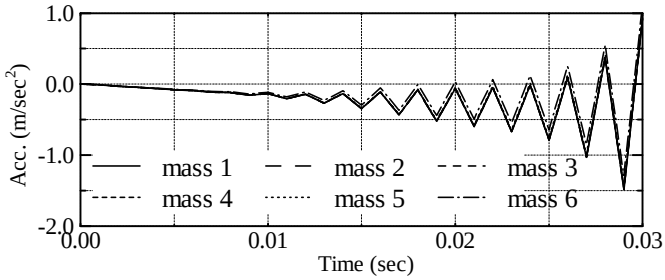

Figure 2.5 Calculation errors of relative response accelerations in case of b=1/2

shows the maximum calculation errors at the top mass, obtained under the assumption that the re-sponse acceleration in the case of b=0 and Δt= 10,000 is exact. In the cases of Δt=1/100 and b>1/4, if b becomes large, the accuracy decreases. However, in the cases of Δt=1/1000 and 1/10,000, even if b is set to be 10, the accuracy is still good, because Δt is small enough compared with the eigen period. The same properties are recognized in the backward calculation. However, as shown in Figs.2.4, when b is set to larger value, the calculation error in the low frequency component becomes large.

On the other hand, it is considered that the solution is divergent in case of small b because Eq.(7) cannot be solved. The condition numbers of the coefficient matrix, $\boldsymbol{A}$ in Eq.(8), are the order of 10^8 in the cases of b<3. Namely, the suitable range of the backward calculation is narrow because of the significant error in case of large b and the divergence in case of small b.

3.3 *Effect of location of the observation point*

The effect of location of the observation point is in-vestigated using the same model as previous section as shown in Fig.2.1. Table 3 shows the condition numbers of coefficient matrix $\boldsymbol{A}$ in the case of Δt=1/1000, g=1/2 and b=1/2. The mass number 1 stands for the top mass and 6 the bottom mass.

Table 2 Maximum calculation error in the forward analysis

b	maximum calculation error (%)		
	Δt=1/10.000	Δt=1/1000	Δt=1/100
0	0	2.3×10^{-2}	2.5
1/6	3.8×10^{-4}	1.9×10^{-2}	1.8
1/4	5.7×10^{-4}	3.8×10^{-2}	3.6
1/2	1.1×10^{-3}	9.5×10^{-2}	8.6
1	2.3×10^{-3}	2.1×10^{-1}	18
2	4.5×10^{-3}	4.3×10^{-1}	36
10	2.3×10^{-2}	2.2	112
100	2.3×10^{-1}	20	109

Table 3 Effect of observed location on condition number of coefficient matrix, $\boldsymbol{A}$ in Eq.(8)

observed mass number	condition number
1	716×10^9
2	757×10^7
3	801×10^5
4	846×10^3
5	895×10^1
6	95×10^0

From the analysis mentioned above, we learn the tendency as follows. When the absolute acceleration observed at the bottom mass is concerned, the condition number is much smaller than of the top

mass. In other words, the accuracy becomes better, if the record observed at the lower mass is treated. For example, even in a 20DOF linear system, when the absolute acceleration observed at the top mass is discussed, divergence occurs at several tens time steps. However, when in case of the bottom mass, the incident wave is identified accurately with the maximum calculation error of 0.1%.

4 APPLICATION FOR NON-LINEAR MODEL

The proposed method is applied to the 3DOF non-linear model. Figs.3.1 and 3.2 show the model and non-linear restoring properties, respectively. The same incident wave form is used in the analyses. Fig.3.3 shows the absolute response acceleration wave form at the top mass computed by the forward calculation.

Four cases from Δt=1/50 to 1/10,000 second are analysed. Fig.3.4 shows identified incident wave form in each case. Fig.3.5 shows identified incident motion through 25Hz-low-pass-filter in the case of Δt=1/1000 second. In the case, integration parameter g is set to 1/2 and values of b are decided to mini-mize the maximum calculation error of identified incident acceleration after 25Hz-low-pass-filtering in each case.

In the cases of Δt=1/50 and 1/100, the numerical error vibrates in lower frequency range and it takes longer time to recover the accuracy than other cases,

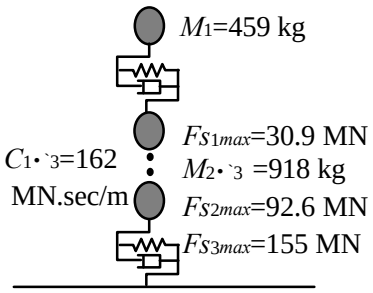

Figure 3.1 Non-linear 3DOF model

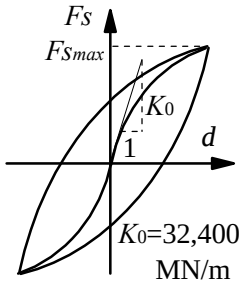

Figure 3.2 Modified Hardin-Drnevich restoring property

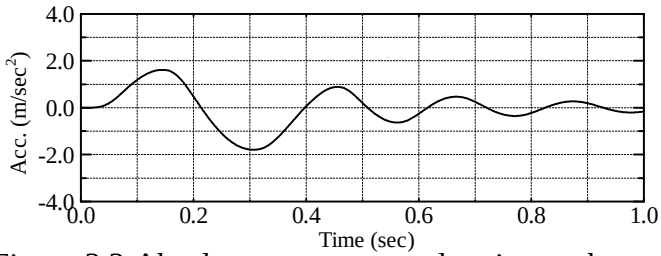

Figure 3.3 Absolute response acceleration at the top mass computed by the forward calculation

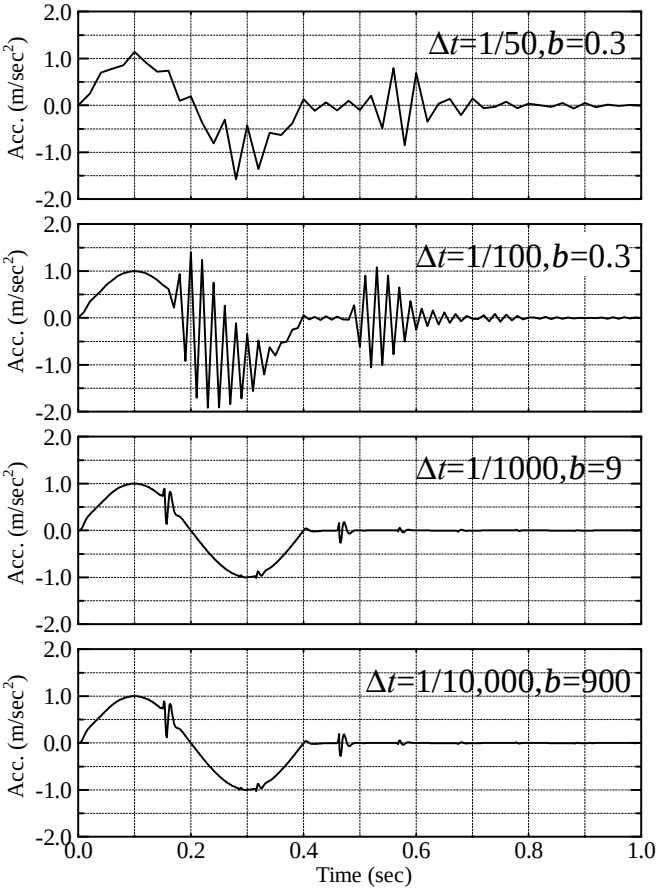

Figure 3.4 Identified incident accelerations

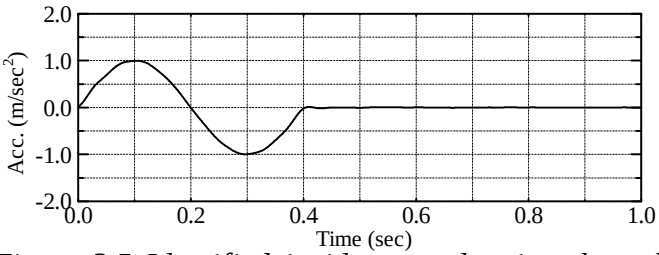

Figure 3.5 Identified incident acceleration through 25Hz-low-pass-filter (Δt=1/1000,b=9)

as shown in Fig.3.4. However, in the cases of Δt= 1/1000 and 1/10,000, the error consists of higher frequency component and the accuracy recovers more quickly than the previous cases. The identified incident accelerations are very accurate, if it is processed by low-pass-filter as shown in Fig.3.5. In other three cases except the case of Δt=1/50, the accurate solutions whose maximum calculation errors are lower than 2.3% are obtained.

5 IMPROVED METHOD

5.1 *Modification by penalty function*

The backward calculation method tends to have the calculation error in the rigid mode. Therefore, $\ddot{x}^{n+1}$

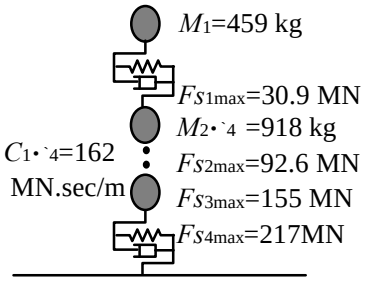

Figure 4.1 Non-linear 4DOF model

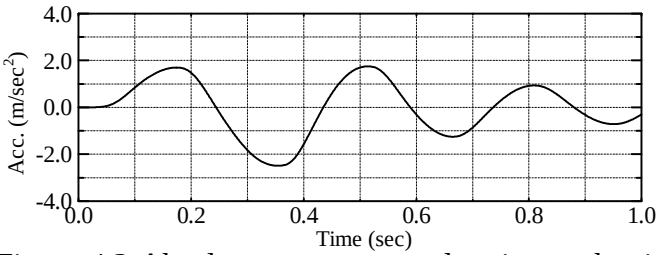

Figure 4.2 Absolute response acceleration at the tip mass computed by the forward calculation

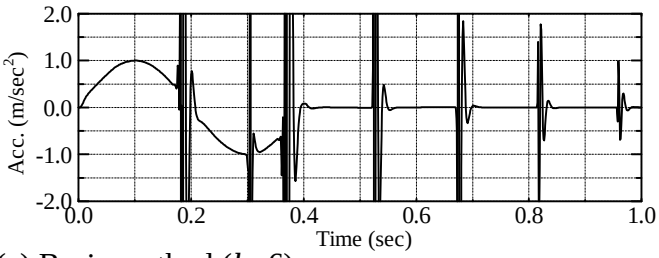

(a) Basic method (b=6)

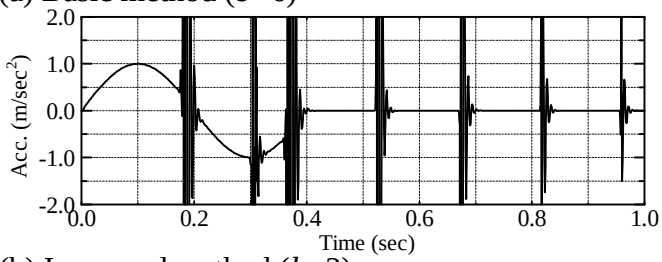

(b) Improved method (b=2)

Figure 4.3 Identified incident acceleration

Table 4 Comparison between maximum calculation error through 25Hz-low-pass-filter by Basic method and that by Improved method

b	Basic method (%)	Improved method (%)
1	255.2	15.7
2	95.3	3.0
3	29.1	3.5
4	11.1	3.8
5	8.4	4.0
6	8.3	4.7
7	8.6	5.6

in Eq.(7) can be improved using a inferred response error of all mass, a, as follows:

$$\ddot{\ddot{x}}_i^{n+1} = \ddot{x}_i^{n+1} + a^{n+1} \tag{10}$$

where subscript i is mass number and • denotes final inferred response at the time step. a^{n+1} can be decided to minimize the following objective function;

$$J = \sum_i^N \sum_j^N M_{ij} \left(\ddot{x}_i^{n+1} + a^{n+1} - \ddot{\ddot{x}}_i^n \right)^2 + r \sum_i^N \sum_j^N M_{ij} \left(a^{n+1} \right)^2 \tag{11}$$

where, mass matrix, M_{ij}, is used as weighting coefficient, and r is a positive constant which controls the calculation error. To distinguish the methods mentioned in chapters 2 and 5, we call the method of chapter 2 "Basic method" and that of chapter 5 "Improved method" hereafter.

5.2 *Numerical example*

The improved method is applied to a 4DOF non-linear system. Modified Hardin-Drnevich model is adopted for non-linear stiffness properties. Fig.4.1 shows the model analysed. Fig.4.2 shows the absolute response acceleration wave form at the top mass computed by the forward calculation excited by the same incident wave as that of the previous analyses shown in Fig.2.2. Seven cases of b=1~7 are analysed. Other parameters are set to Δt=1/1000 second, g=1/2, and r=1. The identified incident wave forms calculated by Basic method and Im-proved method are compared in Figs.4.3(a),(b), respectively. In both methods, significant numerical error is observed for several times in high frequency range. However, the accuracy of identification recovers rapidly. 25Hz-low-pass-filter is applied to eliminate the error in high frequency range from the identified incident wave. Table 4 indicates the maxi-mum calculation errors of the identified incident acceleration by filtering. Figs.4.4(a),(b) show identi-fied wave forms after filtering in the cases of b=6 and 2 for Basic method and Improved method which give the smallest calculation errors. Applying 25Hz-low-pass-filter, the identified wave form of Im-proved method is found to be more accurate than that of Basic method.

It is concluded that Improved method can give more accurate solution than Basic method for every numerical model as it is examined in the previous chapters. The order of the maximum calculation error is less than several percents in the case of Δt=1/1000, b=2 and r=1.

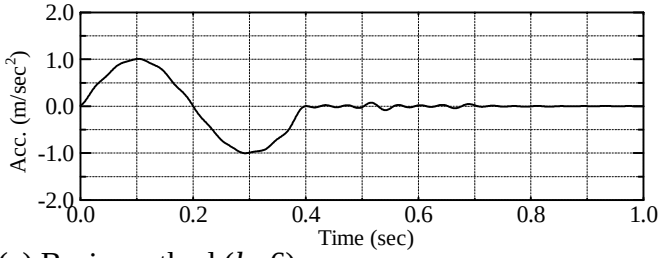

(a) Basic method (b=6)

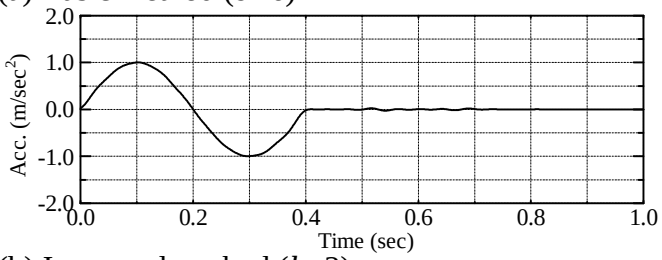

(b) Improved method (b=2)

Figure 4.4 Identified incident acceleration through 25Hz-low-pass-filter

6 CONCLUSION

1. A backward calculation method to identify an incident wave from a recorded acceleration is proposed.
2. The proposed method can identify the incident wave accurately using a linear system with several-DOF and using a non-linear system with small-DOF.
3. The backward calculation method is improved by eliminating the numerical error in rigid mode using penalty function.

REFERENCES

Maruyama,O. & M.Hoshiya 1987. Identification of an input ground motion to a structure. *Proc. of the 19th JSCE Earthquake Engineering Sympo-sium*:145-148. (in Japanese)

Schnabel,P.B., J.Lysmer & H.B.Seed 1972. SHAKE - A computer program for earthquake response analysis of horizontally layered sites. *EERC Report* 72(12), University of California, Berkley

Sudo,A., M.Hoshiya & I.Yanagawa 1995. Identifica-tion of an input and parameters of a MDOF system. *Journal of Structural Engineering* 41A: 709-716. (in Japanese with English Abstract)

Toki,K., T.Sato & J.Kiyono 1989. Identification of structural parameters and input ground motion from response time histories. *Proc. of the Japan Society of Civil Engineers* 410:243-251.